Empirical Relations between Elastic Wavespeeds and Density in the Earth's Crust

Article *in* Bulletin of the Seismological Society of America · December 2005

DOI: 10.1785/0120050077

1 author:

Tom Brocher
United States Geological Survey
262 PUBLICATIONS **7,866** CITATIONS

SEE PROFILE

Bulletin of the Seismological Society of America, Vol. 95, No. 6, pp. 2081–2092, December 2005, doi: 10.1785/0120050077

Empirical Relations between Elastic Wavespeeds and Density in the Earth's Crust

by Thomas M. Brocher

Abstract A compilation of compressional-wave (V_p) and shear-wave (V_s) velocities and densities for a wide variety of common lithologies is used to define new nonlinear, multivalued, and quantitative relations between these properties for the Earth's crust. Wireline borehole logs, vertical seismic profiles, laboratory measurements, and seismic tomography models provide a diverse dataset for deriving empirical relations between crustal V_p and V_s. The proposed V_s as a function of V_p relations fit V_s and V_p borehole logs in Quaternary alluvium and Salinian granites as well as laboratory measurements over a 7-km/sec-wide range in V_p. The relations derived here are very close to those used to develop a regional 3D velocity model for southern California, based on pre-1970 data, and thus provide support for that model. These data, and these relations, show a rapid increase in V_s as V_p increases to 3.5 km/sec leading to higher shear-wave velocities in young sedimentary deposits than commonly assumed. These relations, appropriate for active continental margins where earthquakes are prone to occur, suggests that amplification of strong ground motions by shallow geologic deposits may not be as large as predicted by some earlier models.

Introduction

Seismic wavespeed and density are fundamental properties of earth materials. These properties have been measured in thousands of field and laboratory experiments to, for example, infer the subsurface geometry of geologic units and the average thickness and chemical composition of the earth's crust (e.g., Christensen and Mooney, 1995). For earthquake hazard analyses, regional 3D velocity models used to calculate synthetic strong ground motions in urban areas (e.g., Magistrale *et al.*, 2000) require relations between compressional-wave velocity (V_p), shear-wave velocity (V_s), and density (ρ). For such models V_s is more important than V_p because the larger shear-wave amplitudes mean strong ground motions are more nearly a function of V_s than of V_p (Joyner, 2000).

As seismic tomography and refraction studies usually report only V_p, a direct relation between V_p and V_s is highly desirable. Although V_p/V_s versus V_p has been reported for a variety of sedimentary rocks (Mavko *et al.*, 1998) and for volcanic, igneous, and metamorphic rocks (Christensen, 1996), a single, continuous V_s versus V_p relation has never been reported for the full suite of geologic units that comprise the Earth's crust. This article presents empirical relations among V_p, V_s, and ρ, that can be used to infer V_s for the entire Earth's crust from either V_p or ρ. V_p/V_s is dependent on many factors, including fluid content and bulk chemical composition (e.g., Mavko *et al.*, 1998; also see Discussion), and there is no direct relation between it and V_p. The proposed empirical relations, therefore, are intended to provide a useful average fit between V_s and V_p, much the way that the Nafe–Drake curve (Ludwig *et al.*, 1970) provides an average fit between ρ and V_p.

Data Sources

V_p, V_s, and ρ measurements were compiled from many sources: wireline borehole logs for a variety of rocks, vertical seismic profiles (VSPs) conducted using surface sources and downhole receivers, laboratory or field measurements on hand samples, and *in situ* estimates from seismic tomography studies. Due to the need to update regional velocity models for northern and central California (Brocher *et al.*, 1997a; Stidham *et al.*, 1999), this compilation included a large number of measurements made on California samples.

California borehole data include coincident wireline V_p and V_s logs from (1) Holocene fine-grained sediments in the San Francisco Bay (D. K. Vickery and K. A. Cole, California Dept. of Transportation, written comm., 10 January 1995), (2) Quaternary alluvium in Santa Clara Valley in boreholes up to 410 m deep (Newhouse *et al.*, 2004), (3) Miocene sedimentary rocks from central California (De *et al.*, 1994), and (4) Salinian terrane granites and granodiorites in the SAFOD Pilot Hole at Parkfield (Boness and Zoback, 2004).

VSP data were obtained for (1) a variety of lithologies sampled in 30-m-deep boreholes (Boore, 2003), (2) Miocene sedimentary strata from the Varian well at Parkfield (Daley and McEvilly, 1990), and (3) the Cretaceous Franciscan Complex at The Geysers (Majer *et al.*, 1988).

Ultrasonic laboratory measurements at various confining pressures include (1) averages for various types of sandstones and carbonates (Mavko *et al.*, 1998); (2) individual measurements on a variety of sandstones (Castagna *et al.*, 1985); (3) measurements on Paleozoic sedimentary rocks, mainly carbonates, from the eastern United States (Johnson and Christensen, 1992); (4) individual measurements on welded and nonwelded volcanic tuffs from Yucca Mountain, Nevada (Martin *et al.*, 1994, 1995; Price *et al.*, 1994); (5) individual measurements for basic and other ophiolitic rocks from northern California, including peridotites having varying degrees of serpentinization (Christensen, 1966, 1978; N. I. Christensen, written comm., 1997); (6) individual measurements of metagraywackes and mafic rocks from the Olympic Peninsula and the Puget Lowland (Brocher and Christensen, 2001); (7) individual measurements of metavolcanic and igneous rocks from the south-central Alaska (Brocher *et al.*, 2004); (8) individual measurements of two tonalite samples from the Sierra Nevada (Fliedner *et al.*, 2000), and (9) global averages of hundreds of laboratory measurements of crystalline rocks (Christensen, 1996).

Other data from the San Francisco Bay Area included (1) V_p/V_s and V_p from the seismic tomography model (Boatwright *et al.*, 2004), and (2) V_p and V_s for a velocity model (GIL7) used to model earthquake waveforms (Baise *et al.*, 2003).

Density as a Function of V_p

Existing ρ as a function of V_p relations were used to convert between other relations discussed here. For all rocks excepting mafic crustal and calcium-rich rocks, I used Ludwig *et al.*'s (1970) nonlinear ρ as a function of V_p relation (handpicked V_p and ρ values in Table 1 and Fig. 1). Ludwig *et al.* (1970) present this relation graphically and do not provide an equation. The following new polynomial regression fit to the handpicked ρ and V_p values in Table 1 is valid for V_p between 1.5 and 8.5 km/sec:

$$\rho(\mathrm{g/cm^3}) = 1.6612V_p - 0.4721V_p^2 + 0.0671V_p^3 - 0.0043V_p^4 + 0.000106V_p^5. \quad (1)$$

Equation (1) is the Nafe–Drake curve, previously published only graphically (Ludwig *et al.*, 1970).

Several other empirical ρ values as a function of V_p relations are compared to the Nafe–Drake curve in Figure 1. Gardner's rule (Gardner *et al.*, 1974), derived for sedimentary rocks, is valid for $1.5 < V_p < 6.1$ km/sec:

$$\rho(\mathrm{g/cm^3}) = 1.74V_p^{0.25}. \quad (2)$$

Gardner's rule yields ρ that are generally 0.1 g/cm^3 or less higher than the Nafe–Drake curve, but deviates more substantially from the Nafe–Drake curve for V_p less than 2 km/sec.

Christensen and Mooney (1995) proposed a widely used linear ρ as a function of V_p relation for crystalline rocks:

$$\rho(\mathrm{g/cm^3}) = 0.541 + 0.3601V_p. \quad (3)$$

This relation is appropriate for all rocks (except volcanic and monomineralic rocks) at 10 km depth and is defined for V_p between 5.5 and 7.5 km/sec. For V_p greater than 6 km/sec, this relation yields ρ up to 0.15 g/cm^3 higher than the Nafe–Drake curve (Fig. 1).

Godfrey *et al.* (1997) proposed a separate linear ρ as a function of V_p relation for basalt, diabase, and gabbro, based on measurements reported by Christensen and Mooney (1995) for a depth of 10 km. This relation is valid for V_p between 5.9 and 7.1 km/sec:

$$\rho(\mathrm{g/cm^3}) = 2.4372 + 0.0761V_p. \quad (4)$$

This relation is subparallel to and deviates up to 0.2 g/cm^3 from the Nafe–Drake curve (Fig. 1).

Finally, Figure 1 plots the global average for serpentinites at 10 km (Christensen and Mooney, 1995). This average plots directly on the Nafe–Drake curve.

V_p as a Function of Density

I also regressed the handpicked V_p and ρ values in Table 1 (Ludwig *et al.*, 1970) to derive a new relation for V_p as a function of ρ:

$$V_p(\mathrm{km/sec}) = 39.128\rho - 63.064\rho^2 + 37.083\rho^3 - 9.1819\rho^4 + 0.8228\rho^5, \quad (5)$$

yielding an $R^2 = 0.999$. This relation is accurate for ρ between 2 and 3.5 g/cm^3.

V_s as a Function of V_p

Regression of V_p and V_s observations in Figure 2 for all lithologies except calcium-rich and mafic rocks, gabbros, and serpentinites yielded the following new empirical relationship for V_s as a function of V_p:

$$V_s(\mathrm{km/sec}) = 0.7858 - 1.2344V_p + 0.7949V_p^2 - 0.1238V_p^3 + 0.0064V_p^4. \quad (6)$$

I will refer to equation (6) as "Brocher's regression fit." It fits the data with an $R^2 = 0.979$ for V_p between 1.5 and 8 km/sec. Although this regression did not include V_s and V_p values from a seismic tomography model along the Haywood fault (Hardebeck *et al.*, 2004), it fits those values well

Table 1
Empirical V_p, V_s, Density, σ, and V_p/V_s Relations

V_p (km/sec)	Equation (11) V_s (km/sec)	Equation (12) V_s (km/sec)	Equation (6) V_s (km/sec)	Equation (1) Density (gm/cc)	Equation (11) Poisson's Ratio	Equation (12) Poisson's Ratio	Equation (11) V_p/V_s	Equation (12) V_p/V_s
1.50	0.19	0.13	0.34	1.55	0.492	0.496	7.969	11.787
1.75	0.40	0.46	0.46	1.83	0.472	0.463	4.342	3.799
2.00	0.64	0.69	0.61	1.95	0.442	0.432	3.102	2.894
2.25	0.88	0.90	0.79	2.03	0.409	0.405	2.548	2.497
2.50	1.12	1.10	0.98	2.10	0.375	0.380	2.236	2.270
2.75	1.34	1.30	1.19	2.15	0.343	0.357	2.046	2.123
3.00	1.56	1.49	1.41	2.22	0.314	0.338	1.920	2.020
3.25	1.76	1.67	1.63	2.26	0.292	0.320	1.845	1.945
3.50	1.96	1.85	1.86	2.31	0.272	0.305	1.787	1.888
3.75	2.14	2.03	2.07	2.35	0.260	0.292	1.756	1.845
4.00	2.31	2.21	2.28	2.38	0.250	0.281	1.732	1.812
4.25	2.47	2.38	2.48	2.42	0.244	0.272	1.718	1.786
4.50	2.64	2.55	2.67	2.45	0.239	0.264	1.708	1.767
4.75	2.79	2.71	2.85	2.49	0.236	0.258	1.701	1.752
5.00	2.95	2.87	3.01	2.53	0.233	0.254	1.695	1.741
5.25	3.11	3.03	3.16	2.57	0.231	0.251	1.691	1.734
5.50	3.25	3.18	3.30	2.62	0.232	0.249	1.693	1.730
5.75	3.39	3.33	3.43	2.66	0.233	0.248	1.695	1.728
6.00	3.52	3.47	3.55	2.71	0.238	0.248	1.705	1.728
6.25	3.65	3.61	3.66	2.76	0.242	0.249	1.714	1.730
6.50	3.75	3.75	3.77	2.81	0.250	0.251	1.732	1.733
6.75	3.87	3.88	3.88	2.87	0.255	0.253	1.744	1.738
7.00	3.99	4.01	4.00	2.93	0.259	0.255	1.753	1.744
7.25	4.12	4.14	4.12	3.02	0.262	0.258	1.761	1.751
7.50	4.25	4.27	4.26	3.10	0.263	0.261	1.763	1.758
7.75	4.38	4.39	4.42	3.18	0.265	0.264	1.769	1.765
8.00	4.52	4.51	4.61	3.27	0.265	0.267	1.769	1.773
8.25	4.66	4.64	4.84	3.35	0.265	0.269	1.769	1.779
8.50	4.81	4.76	5.10	3.45	0.265	0.271	1.769	1.785

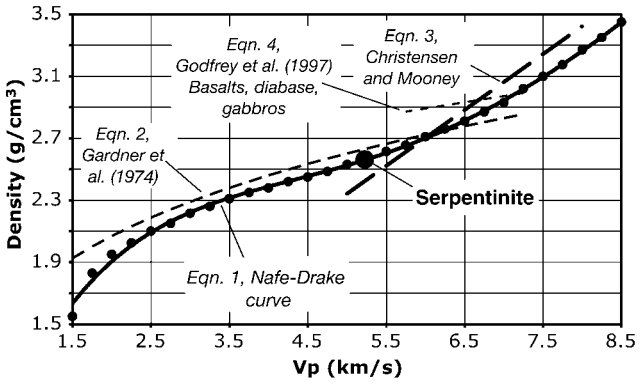

Figure 1. Comparison of published density versus V_p relations used here. Filled circles show handpicked values from the curve published by Ludwig *et al.* (1970). Solid line (equation 1), the Nafe–Drake curve (Ludwig *et al.*, 1970), shows a polynomial regression to these picks and is the preferred density versus V_p relation. Other labeled lines show relations discussed in the text.

(Fig. 2). "Brocher's regression fit" (equation 6) provides a useful fit to observed V_s within the crust for V_p between 1.5 and 7.5 km/sec.

Figure 2 demonstrates a rapid increase in V_s with V_p. Measurements in shallow boreholes for young, saturated sediments having a V_p close to 1.5 km/sec yield V_s close to 0.1 km/sec (D. K. Vickery and K. A. Cole, California Dept. of Transportation, written comm., 10 January 1995; Boore, 2003). For Quaternary alluvium and older sedimentary rocks, having V_p between 1.5 and 2.5 km/sec a rapid increase in V_s is constrained by wireline logs (De *et al.*, 1994; Newhouse *et al.*, 2004). For still older or coarser-grained sedimentary rocks, having V_p between 2.5 and 3.5 km/sec, V_s further increases based on VSP data from The Geysers and Parkfield (Majer *et al.*, 1988; Daley and McEvilly, 1990), averages for laboratory measurements on sedimentary rocks and volcanic tuffs (Martin *et al.*, 1994, 1995; Price *et al.*, 1994; Mavko *et al.*, 1998), and tomography data (Boatwright *et al.*, 2004).

For V_p between 1.5 and 4.25 km/sec the data in Figure 2 are also consistent with a linear regression of borehole and VSP measurements for clay-rich sedimentary rocks derived by Castagna *et al.* (1985):

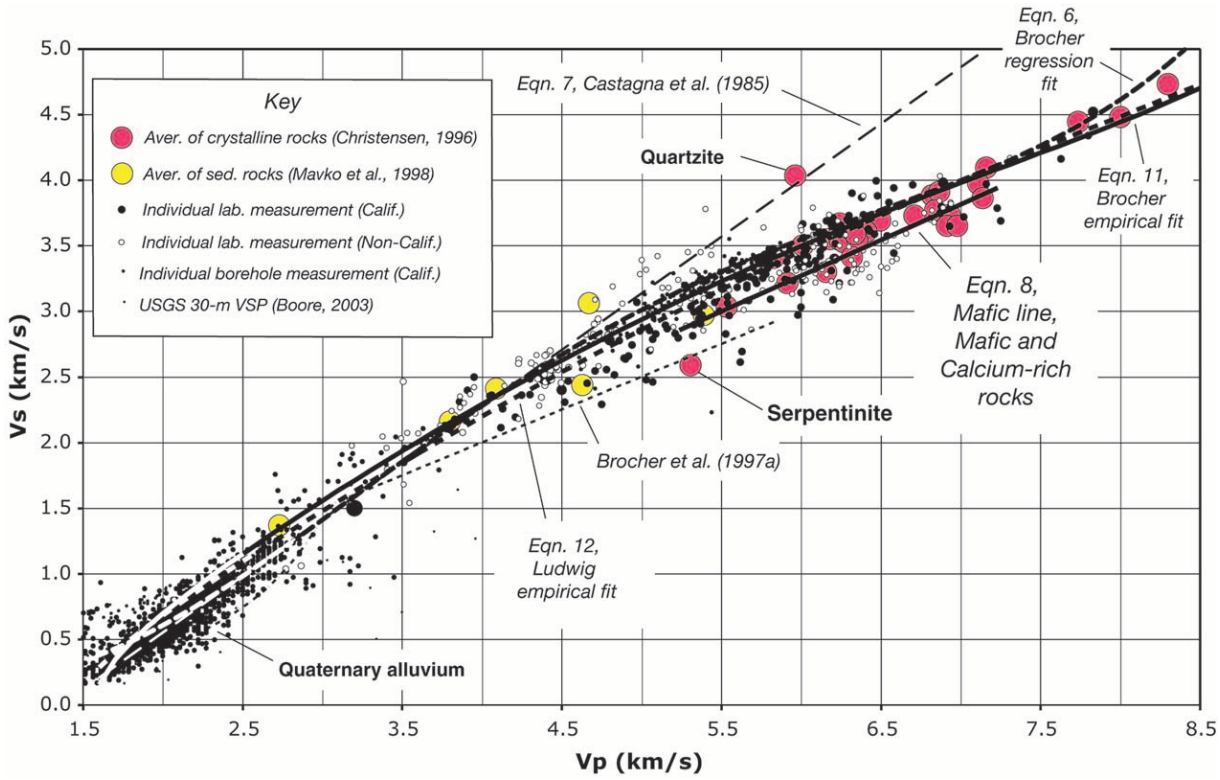

Figure 2. V_s as a function of V_p for common lithologies. Solid circles represent samples from northern and central California; unfilled circles represent other samples. Circle sizes increase qualitatively with data quality (see key): largest sizes represent averages of tens of individual laboratory measurements, intermediate sizes show individual laboratory measurements, small sizes correspond to individual borehole measurements, and the smallest sizes correspond to USGS 30-m VSPs. Data sources are identified in Figure 3 and Table 2. Values reported by a seismic tomography model along the Hayward fault (Hardebeck *et al.*, 2004), for V_p between 4 and 7 km/sec, are shown as filled circles. Various V_s as a function of V_p relations discussed in the text are compared to the data and to each other.

$$V_s(\text{km/sec}) = (V_p - 1.36)/1.16. \quad (7)$$

This so-called mudline overpredicts V_s for V_p above 4.25 km/sec (Fig. 2).

V_s for calcium-rich rocks (including dolomites and anorthosites), mafic rocks, and gabbros lie 0.2 to 0.3 km/sec below the general trend of the data in Figure 2. For these units, I introduce a separate new linear relation, here called, for brevity, the "mafic line":

$$V_s(\text{km/sec}) = 2.88 + 0.52(V_p - 5.25), \quad \text{defined for } 5.25 < V_p < 7.25 \text{ km/sec}. \quad (8)$$

Christensen (1996), among many others, reported that serpentinites have an anomalously low V_s. Christensen's (1996) global average for confining pressures of 200 MPa plots about 0.5 km/sec below the general trend of the observations (Fig. 2).

V_p as a Function of V_s

The data used to derive "Brocher's regression fit" (equation 6) were also regressed for V_p as a function of V_s. Regression of these observations (which excluded calcium-rich and mafic rocks, gabbros, and serpentinites) yielded the following new empirical regression relationship between V_p and V_s:

$$V_p(\text{km/sec}) = 0.9409 + 2.0947V_s - 0.8206V_s^2 + 0.2683V_s^3 - 0.0251V_s^4. \quad (9)$$

This regression, valid for V_s between 0 and 4.5 km/sec, fits the data in Figure 2 with $R^2 = 0.962$.

Poisson's Ratio as a Function of V_p

Figure 3 replots the observations of V_p and V_s in terms of Poisson's ratio versus V_p. Poisson's ratio, σ, is related to the ratio of V_p and V_s by

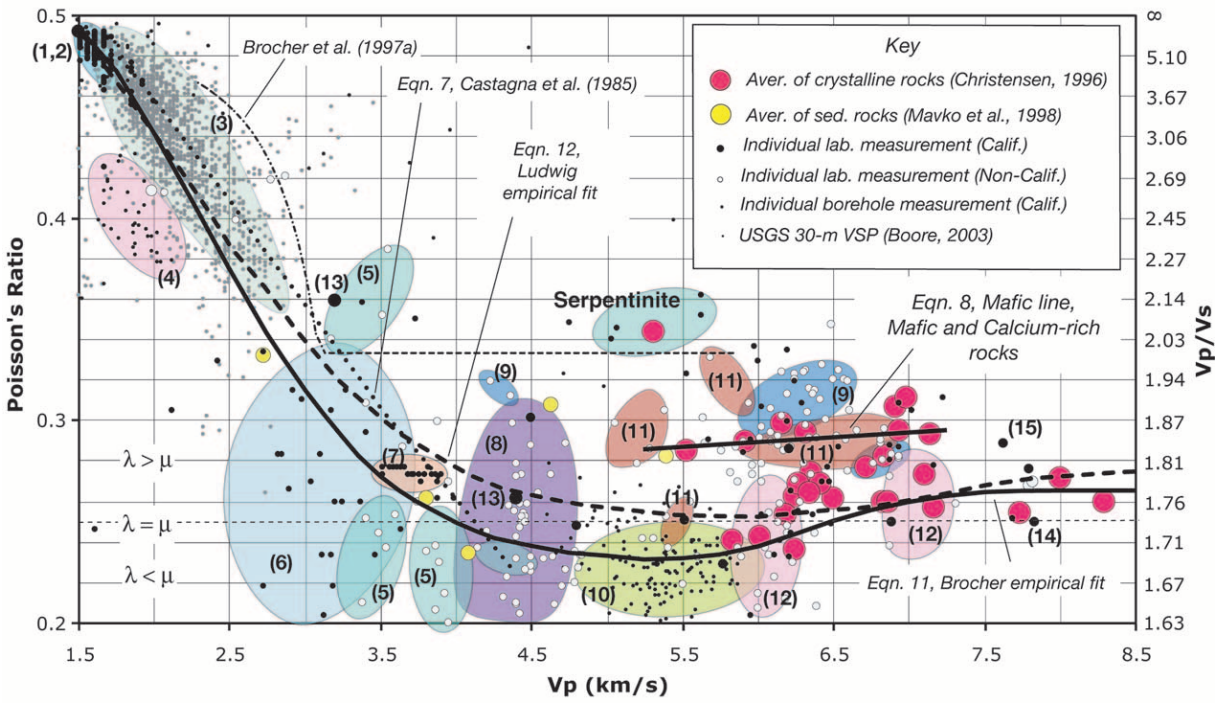

Figure 3. Poisson's ratio as a function of V_p for common lithologies. Colored ellipses highlight measurements reported by a single reference: bold numbers in parentheses link ellipses (and some isolated measurements) to references provided in Table 2. Thinner horizontal dashed line shows Poisson's ratio of 0.25 ($V_p/V_s = 1.73$) commonly assumed for the crust when the first Lame constant, λ, equals the shear modulus, μ.

$$\sigma = 0.5[(V_p/V_s)^2 - 2]/[(V_p/V_s)^2 - 1]. \quad (10)$$

Poisson's ratio is simply another means of relating V_p and V_s, and it contains no independent information. Crustal rocks are frequently assumed to have a Poisson's ratio of 0.25, which is the case when the first Lamé constant equals the shear modulus. Plotting Poisson's ratio in Figure 3, however, makes it is possible to better distinguish between the data sources used in this study (Table 2).

For rocks typical of the upper and middle crust having V_p between 4 and 6.5 km/sec, Poisson's ratio in northern California is less than 0.25 (Fig. 3). These low Poisson's ratios are attributed to the high quartz contents of these rocks: quartz has an anomalously low Poisson's ratio (σ = 0.10) (Christensen, 1996). In northern California the low Poisson's ratios for this range of V_p reflect the high quartz content of its sandstones, volcanic tuffs, metagraywackes of the Franciscan complex, granites and granidiorites of the Salinian terrane, granite gneiss, and biotite gneiss (Christensen, 1996).

For rocks of the lower crust and upper mantle having V_p higher than 6.5 km/sec, Poisson's ratio increases slowly between 0.25 and 0.28. These rocks correspond to greenschist facies basalts, diorites, mafic garnite granulites, pyroxenites, eclogites, peridotite, and dunites (Christensen, 1996). Thus, high Poisson's ratios in the crust for V_p above 6.5 km/sec do not necessarily imply the presence of fluids, as is often speculated.

A new empirical Poisson's ratio versus V_p relation was fit manually to the data in Figure 3 and is defined for V_p between 1.5 and 8.5 km/sec:

$$\sigma = 0.8835 - 0.315V_p + 0.0491V_p^2 - 0.0024V_p^3. \quad (11)$$

Equation (11) excludes data for calcium-rich and mafic rocks, which are separately fit by the mafic line (equation 8; Table 3). I shall call equation (11) "Brocher's empirical fit" as a reminder that it was fit by eye. Fitting this smooth curve through scattered data emphasized averages of laboratory measurements (Christensen, 1996; Mavko *et al.*, 1998), borehole logging (Daley and McEvilly, 1988; Boness and Zoback, 2004; Newhouse *et al.*, 2004), and tomography data (Boatwright *et al.*, 2004), thought to be the most accurate.

Finally, Figure 3 plots a relation derived from Ludwig *et al.* (1970), using their empirical Poisson's ratio versus ρ curve and equation (5). Ludwig *et al.* (1970) present their relation graphically. I hand digitized their curve and regressed a polynomial to these handpicked points. I refer to this relation as "Ludwig's empirical fit," which is valid for V_p between 1.5 and 8.5 km/sec:

$$\sigma = 0.769 - 0.226V_p + 0.0316V_p^2 - 0.0014V_p^3. \quad (12)$$

Table 2
Identity of Samples Labeled in Figures 3 and 4

Figure	Data Type	Lithology	Reference
1	Borehole log	Holocene sediments	Vickery and Cole written comm. (1985)
2	VSP	Varied	Boore (2003)
3	Borehole log	Quaternary alluvium	Newhouse *et al.* (2004)
4	Borehole log	Sedimentary rocks	De *et al.* (1994)
5	Borehole log and VSP	Sedimentary rocks	Castagna *et al.* (1985)
6	VSP	Sedimentary rocks	Daley and McEvilly (1990)
7	VSP	Franciscan Complex	Majer *et al.* (1988)
8	Laboratory	Yucca Mountain tuffs	Martin *et al.* (1994, 1995), Price *et al.* (1994)
9	Laboratory	Sedimentary rocks	Johnson and Christensen (1992)
10	Borehole log	Salinian granite	Boness and Zoback (2004)
11	Laboratory	Metagraywackes and mafic rocks	Brocher and Christensen (2001)
12	Laboratory	Metamorphic rocks	Brocher *et al.* (2004)
13	Tomography	Upper crust	Boatwright *et al.* (2004)
14	Velocity Model	Crust	Baise *et al.* (2003)
15	Laboratory	Mafic rocks	Christensen (1966, 1978)

Table 3
Empirical Relation for Mafic and Calcium-Rich Rocks

V_p (km/scc)	V_s (km/scc)	Density (gm/cc)	Poisson's Ratio	V_p/V_s
5.25	2.88	2.57	0.285	1.824
5.50	3.01	2.62	0.286	1.827
5.75	3.14	2.66	0.287	1.831
6.00	3.27	2.71	0.289	1.834
6.25	3.40	2.76	0.290	1.838
6.50	3.53	2.81	0.291	1.842
6.75	3.66	2.87	0.292	1.846
7.00	3.79	2.93	0.293	1.849
7.25	3.91	3.02	0.295	1.853

Equations (11) and (12) are nearly identical and deviate most for V_p between 3 and 6 km/sec (Fig. 3).

Poisson's Ratio as a Function of Density

A Poisson's ratio versus ρ relation was calculated (Fig. 4, Table 1) using the Nafe–Drake curve and Brocher's empirical fit (equation 11). Figure 4 compares this relation against Ludwig *et al.*'s (1970) and tests both relations against measurements from northern California.

Both relations are comparable for ρ typical of younger sedimentary rocks and deposits up to 2.0 g/cm^3 (Fig. 4). For ρ close to 1.5 g/cm^3, both relations match measurements for fine-grained sediments in the San Francisco Bay area (D. K. Vickery and K. A. Cole, written comm., 10 January 1995; Boore, 2003). Poisson's ratio decreases only gradually for ρ between 1.5 and 1.8 g/cm^3. For ρ typical of older sedimentary rocks and the uppermost basement rocks, between 2.1 and 2.7 g/cm^3, Poisson's ratios predicted by Brocher's empirical fit are slightly lower than Ludwig *et al.'s* (1970) yet predict V_s values that are no more than 0.1 km/sec higher (Fig. 4). For ρ typical of crystalline rocks in the middle to lower crust and upper mantle, above 2.7 g/cm^3, both relations are comparable and fit measurements for a variety of metamorphic, igneous, and volcanic rocks (Christensen, 1996).

Fits to V_p and V_s Provided by the Empirical Relations

This section compares the fits provided by several of the equations presented here to the V_s and V_p data from northern California, and to global averages of V_s and V_p measurements in basement rocks. Taken as a whole, these datasets represent the full range of V_p investigated here and each samples an important northern California lithology. Borehole V_p and V_s suspension logs in Santa Clara Valley sample Quaternary alluvium (Newhouse *et al.*, 2004), an important unit for forecasting strong ground motions there (Frankel and Vidale, 1992; Joyner, 2000). V_p and V_s suspension logs from the SAFOD Pilot Hole sample Salinian granite (Boness and Zoback, 2004). Christensen (1996) reported global averages of laboratory V_s and V_s measurements for many lithologies, including several that comprise the majority of the crystalline crust in Northern California (metagraywacke, granite, basalt, gabbro, and serpentinite).

Five boreholes in the Santa Clara Valley (Fig. 5), each penetrating about 300 m, provide both V_p and V_s suspension logs in Quaternary alluvium (CCOC, GUAD, MCGY, STGA, and STPK) (Newhouse *et al.*, 2004). V_s was calculated from the observed V_p logs using the mudline (equation 7), Brocher's empirical fit (equation 11), and Ludwig's empirical fit (equation 12) (Fig. 6). For these wells, V_s predicted from the observed V_p ogs using the mudline best match the observed V_s logs with an average standard deviation of 0.1 km/sec (Fig. 6). The V_s logs predicted by the mudline provide a surprisingly close fit to the peaks and troughs on the observed logs that correspond to coarser and finer grained units within the alluvium. These close fits for V_p greater than 1.49 km/sec were achieved using V_p suspension logs starting at about 40-km depth to total well depths between 250 and 410 m. The mudline generally predicted V_s values that

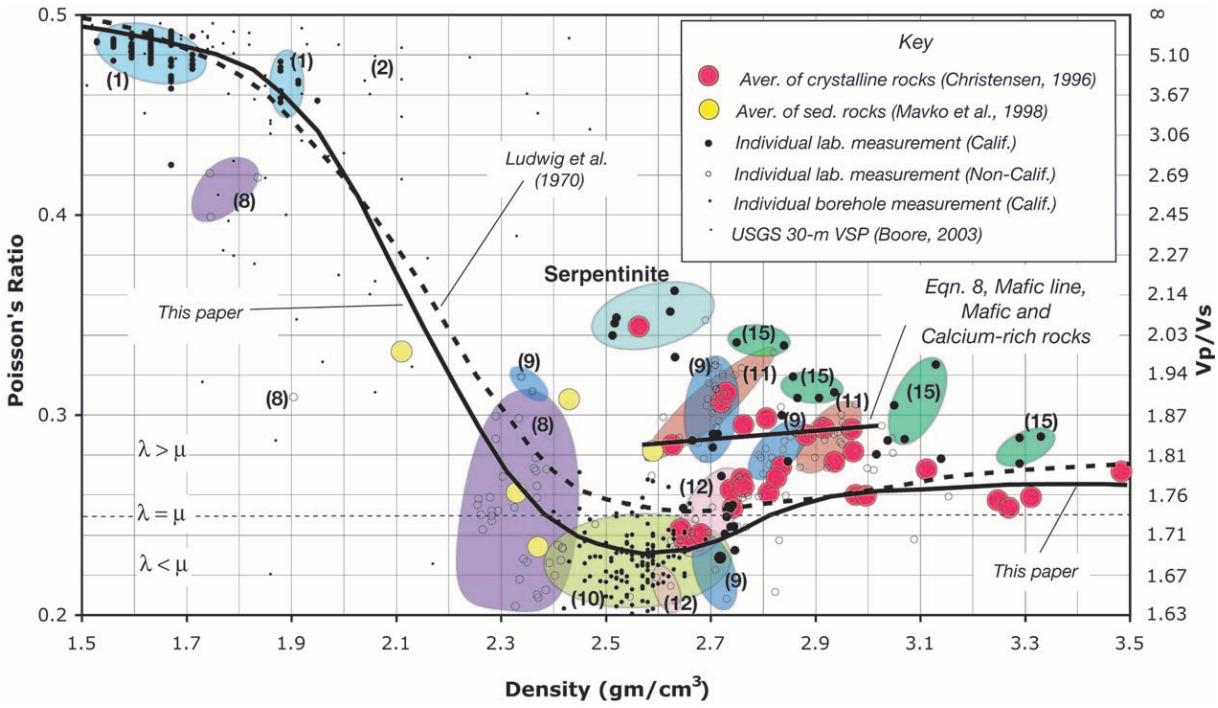

Figure 4. Poisson's ratio as a function of density for common lithologies. Format as for Figure 3.

ranged from 0.006 to 0.091 km/sec too low; only at CCOC did it overpredict V_s on average.

Observed V_s logs from Santa Clara Valley were also compared to V_s predicted using Ludwig's empirical fit (equation 12). Ludwig's empirical fit consistently overestimated the observed V_s in the five boreholes by an average of 0.096 km/sec at depths greater than 40 m. It overpredicted V_s the most at CCOC, near the center of the valley, by an average of 0.17 km/sec. Ludwig's empirical fit was most accurate at MCGY, near the western margin of Santa Clara Valley, where it overpredicted V_s by an average of 0.04 km/sec.

Brocher's empirical fit (equation 11) was the least accurate relation for these Santa Clara Valley boreholes, as it consistently overpredicted V_s. At CCOC, Brocher's empirical fit overpredicted V_s by an average of 0.20 km/sec. At MCGY, it overpredicted V_s by an average of 0.06 km/sec.

The mudline, Brocher's empirical fit, and Ludwig's empirical fit all provide significantly closer fits than the simple depth dependent velocity function for Plio-Quaternary deposits used by Brocher *et al.* (1997a). Figure 6 indicates that the relation used by Brocher *et al.* (1997a) underpredicts V_s in these deposits by a factor of 2 to 3 in the lowermost parts of these 300-m-deep wells. Models based on either the mudline, Brocher's empirical fit, or Ludwig's empirical fit predict lower amplifications than those produced by the Brocher *et al.* (1997a) model.

For the higher values of V_p and V_s reported in borehole logs from the SAFOD pilot hole (Boness and Zoback, 2004), the relative accuracy of the empirical relations is reversed (Fig. 7). There the mudline (equation 7) overpredicts V_s by an average of 0.27 km/sec (and is not shown). In contrast, Brocher's empirical fit (equation 11) and Ludwig's empirical fit (equation 12) underpredict V_s by an average of 0.03 and 0.01 km/sec, respectively (Fig. 7), and each yield standard deviations of 0.12 km/sec Thus, Brocher's empirical fit and Ludwig's empirical fit should yield useful approximations for V_s in Salinian granite (Fig. 7), but the mudline will substantially overpredict V_s. The simple depth dependent velocity function used by Brocher *et al.* (1997a) for Salinian granites fits the average V_s for the SAFOD Pilot Hole to within 0.06 km/sec. (Fig. 7).

V_s calculated from Brocher's regression fit (equation 6), the mafic line (equation 8), and Ludwig's empirical fit (equation 12) are compared in Figure 8 to laboratory measurements of V_p and V_s at 200 MPa confining pressure (Christensen, 1996). One should expect a close fit to equations (6) and (8), as these measurements were used to derive them. Average misfits produced by Brocher's regression fit to Figure 8A are less than 0.08 km/sec; average misfits of Ludwig's empirical fit in Figure 8A are less than 0.01 km/sec. The predictions of the mafic line (equation 8) to mafic rocks, gabbros, and calcium-rich rocks in Figure 8B are also close, yielding an average misfit less than 0.02 km/sec.

Implications for 3D Velocity Models for the San Francisco Bay Area

Stidham *et al.* (1999) used a simplified model for the Cenozoic basins in the San Francisco Bay Area to construct a regional 3D velocity model that they used to investigate

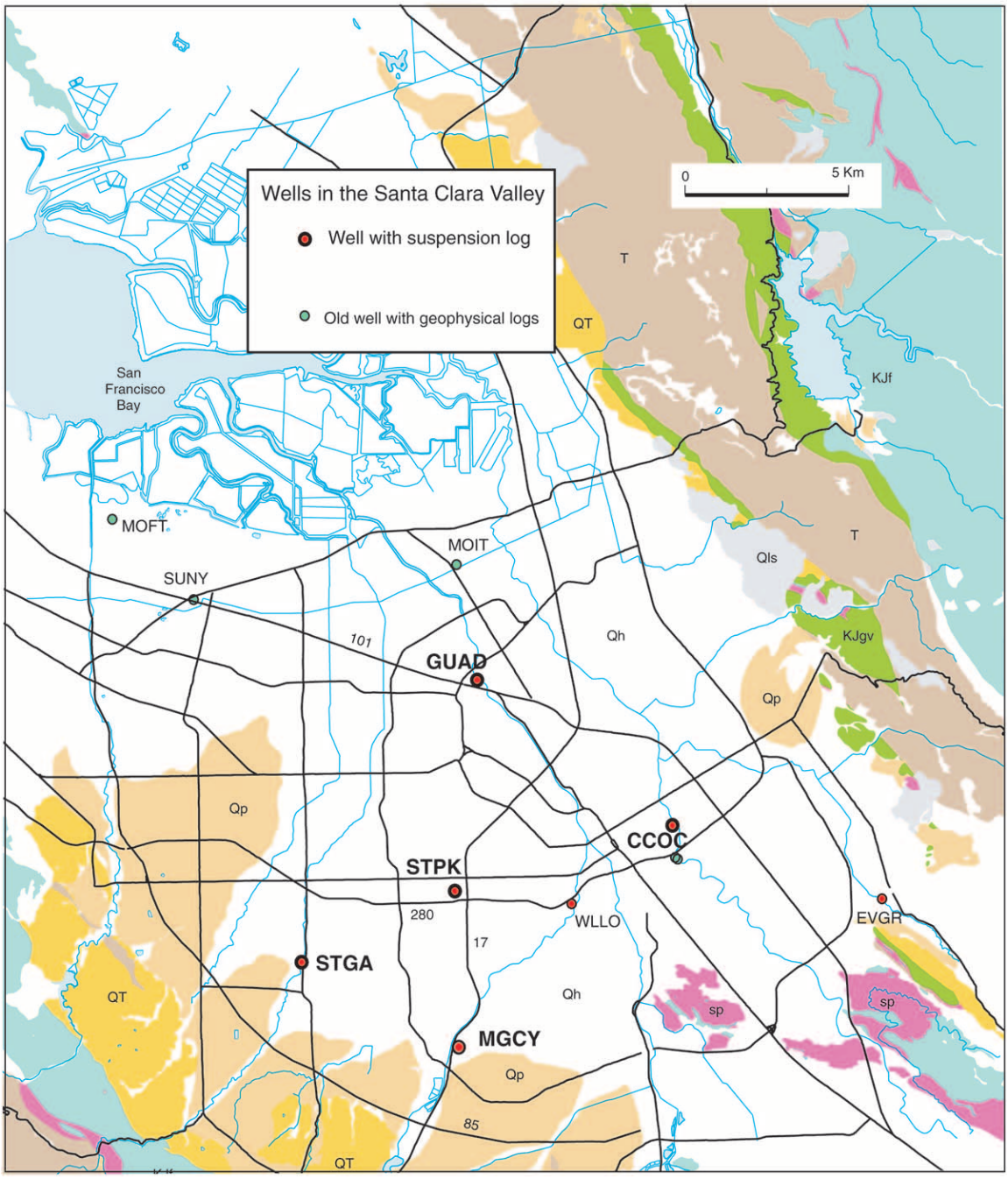

Figure 5. Geologic map showing locations of 300-m to 400-m-deep boreholes in Santa Clara Valley, south of San Francisco Bay, for which both V_p and V_s suspension logs were run within the Quaternary alluvium. Modified from Newhouse *et al.* (2004). Qh, Holocene age deposits; Qls, Holocene and Pleistocene landslide deposits; Qp, Late-Pleistocene-age deposits; QT, Pliocene-Quaternary age sedimentary deposits (Santa Clara Formation and equivalents); KJf, Franciscan Assemblage; KJgv, Great Valley Sequence; sp, serpentinite and associated Coast Range ophiolite; T, Tertiary-age sedimentary deposits (includes some volcanics and the Monterey Formation).

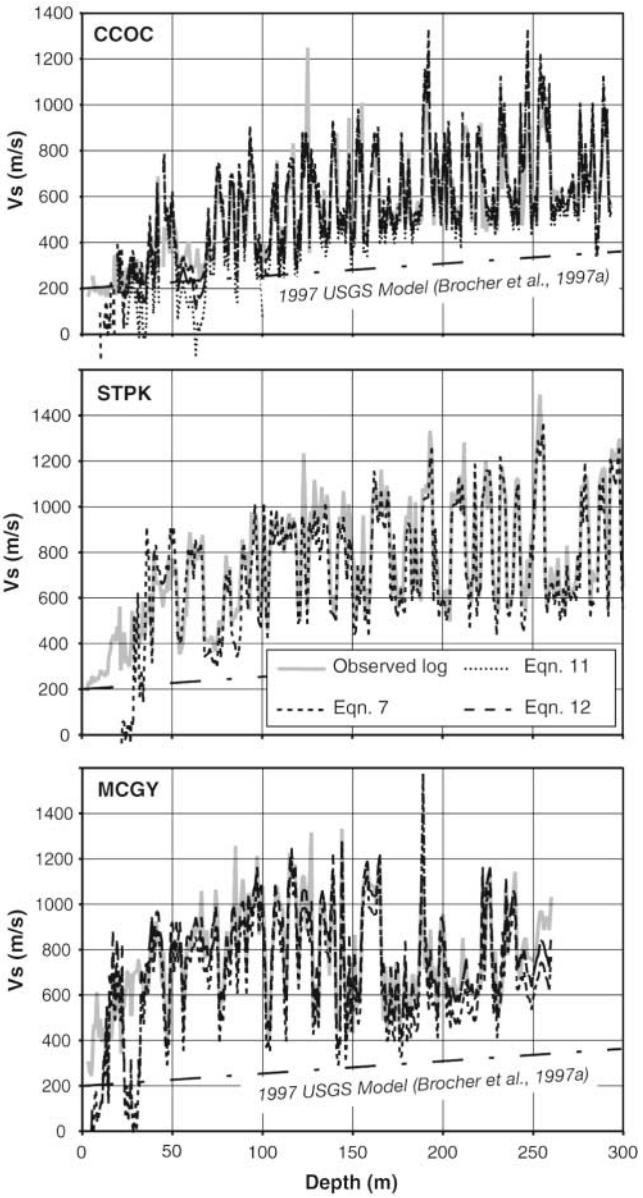

Figure 6. Comparison of the observed V_s (heavy solid line) for three borehole suspension logs from the Santa Clara Valley versus V_s predicted from the observed V_p suspension logs from these boreholes. Each log is compared to predictions of the mudline (equation 7) of Castagna *et al.* (1985). For CCOC, I show fit provided by Brocher's empirical fit (equation 11) shifted downward by 0.2 km/sec. For CCOC and MCGY, I show fits provided by Ludwig's empirical fit (equation 12). V_s calculated using Ludwig's empirical fit were shifted down by 0.17 km/sec for the CCOC log and by 0.04 km/sec for the MCGY log. The dash-dot line shows the depth dependent relation for Plio-Quaternary alluvium used by Brocher *et al.* (1997a) in their regional 3D San Francisco Bay Area model.

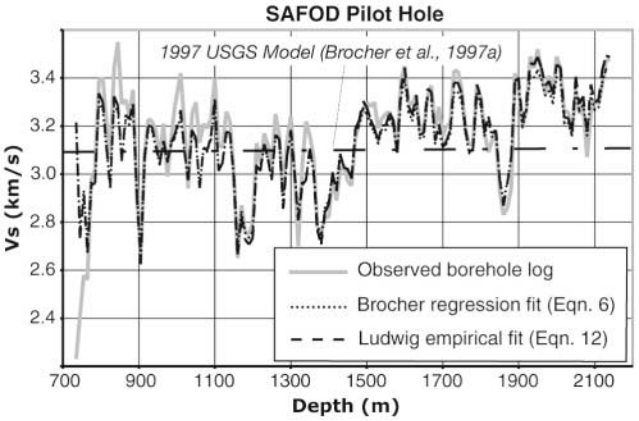

Figure 7. Comparison of observed V_s borehole log from the SAFOD pilot hole (Boness and Zoback, 2004) versus V_s predicted from observed V_p borehole log using Brocher's empirical fit and Ludwig's empirical fit. The dash-dot line shows the depth-dependent relation for Salinian basement used by Brocher *et al.* (1997a) in their regional 3D San Francisco Bay Area model.

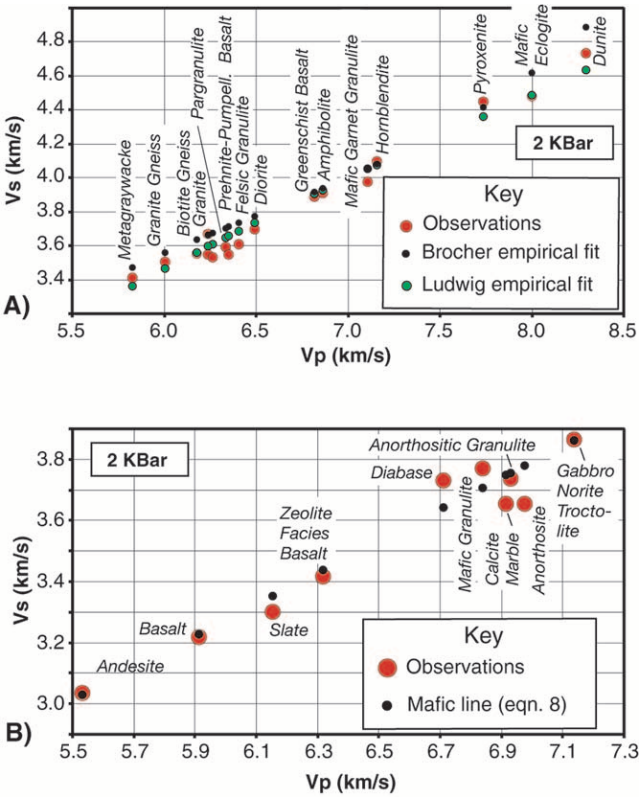

Figure 8. Comparison between laboratory measurements of V_p and V_s for a variety of crystalline rocks at 200 MPa (2 Kbar) confining pressure (Christensen, 1996) versus calculated V_s (A) V_s calculated using Brocher's regression fit and Ludwig's empirical fit. (B) V_s for a variety of mafic rocks, gabbros, and calcium-rich rocks calculated using the mafic line.

the spatial distribution of strong ground motions produced by the 1989 Loma Prieta earthquake. Brocher *et al.* (1997a) developed a more detailed velocity model for these basins using inversions of gravity for basin structure (Jachens *et al.*, 1997), as well as compilations of sonic and density well log data from oil industry boreholes (Brocher *et al.*, 1997b; Tiballi and Brocher, 1998; Brocher, 2005). Subsequent observations of compressional-wave arrival times from local and teleseismic earthquakes by a temporary seismic network deployed in Santa Clara Valley indicate that that the geometry of the Cenozoic basins and the V_p used in the basins there (Brocher *et al.*, 1997a) are reasonably accurate (Fletcher *et al.*, 2003). Fletcher *et al.* (2003) note, however, that V_s used in this model within the basins are too small (or, equivalently, that V_p/V_s is too large). Boatwright *et al.* (2004) also found it necessary to increase the V_s in the basins in the Brocher *et al.* (1997a) model to better match results from V_s inferred from coincident seismic tomography models.

The source of this error is immediately apparent in Figures 2 and 3, which plot the V_s and Poisson's ratio used by Brocher *et al.* (1997a) in the upper 6 km of the Cenozoic basins. Brocher *et al.'s* (1997a) curves lie well off general trends. Because compressional-wave arrival times are matched reasonably accurately by the Brocher *et al.* (1997a) model within Santa Clara Valley, the inaccuracy of the V_s curves used by Brocher *et al.* (1997a) for Plio-Quaternary and older Cenozoic sedimentary deposits (Figs. 2, 3) likely accounts for the failure of their model to adequately match observations of shear-wave arrival travel times in Santa Clara Basin (Fletcher *et al.*, 2003). Substitution of the V_s in the basin models of Brocher *et al.* (1997a) using values calculated from V_p using equations presented here should substantially improve the accuracy of the V_s model in these basins.

Elastic Constants as a Function of V_p and/or Density

Another potential application of the equations presented here is the calculation of Lamé's elastic constants as functions of either V_p or density (Fig. 9). For example, in Figure 9, I calculated Lamé's second constant, μ, the shear modulus, from $\mu = V_s^2 \rho$ (e.g., Telford *et al.*, 1976) using equations (1), (5), (7), and (11). Similarly, I calculated Lamé's first constant, λ, from $\lambda = \rho(V_p^2 - 2V_s^2)$ (e.g., Telford *et al.*, 1976). As reported by Birch (1966), the Lamé constants for crystalline rocks vary between 20 and 100 GPa and increase nonlinearly with V_p and ρ (Fig. 9). Other elastic constants, including the Bulk modulus, K, Youngs modulus, E, and Poisson's ratio, σ, can be readily calculated from these Lamé constants: $K = \lambda + 2/3\mu$, $E = \mu(3\lambda + 2\mu)/(\lambda + \mu)$, and $\sigma = \lambda/[2(\lambda + \mu)]$ (e.g., Telford *et al.*, 1976).

The curves shown in Figure 9 qualitatively illustrate the expected variation of the elastic constants with depth within the crust. For upper crustal velocities, having V_p less than 4 km/sec, λ is much greater than μ, and Poisson's ratios are

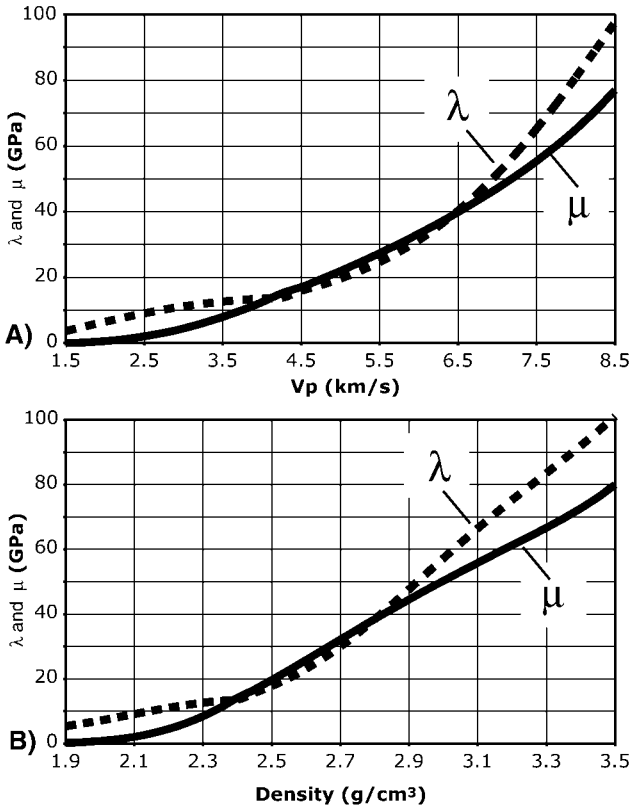

Figure 9. Lamé's parameters plotted as a function of (A) V_p and (B) density calculated using equations (1), (5), (7), and (11). Lamé's second constant, μ, is the shear modulus. Lamé's first constant, λ, is equivalent to the bulk modulus minus $2/3\mu$.

greater than 0.25 (Figs. 3, 9A). For V_p between 4 and 6.5 km/sec, corresponding to most if not all of the middle crust as well as the topmost lower crust, μ equals or is slightly greater than λ (Fig. 9A). Here the Poisson's ratio is slightly less than 0.25 (Fig. 3). For V_p between 6.5 and 8.5 km/sec, within the base of the lower crust and upper mantle, λ is again greater than μ, leading to Poisson's ratios greater than 0.25 (Figs. 3, 9A). A similar relationship is present when these constants are plotted as a function of density (Fig. 9B).

Discussion and Summary

This update to Ludwig *et al.*'s (1970) seminal work compares relations derived from that article to more recently acquired V_p and V_s observations. The generally favorable comparison suggests that using Ludwig *et al.*'s (1970) relation in the SCEC regional 3D community velocity model (Magistrale *et al.*, 2000) should yield accurate V_s. This study differs from that of Ludwig *et al.* (1970) in that it emphasizes northern California samples, more representative of younger tectonic terranes, than do they. Although Ludwig's empirical fit (equation 12) may be more appropriate for the continental crust in general, the relations proposed here (either Brocher's regression fit, Brocher's empirical fit, or the mafic line) may

be more appropriate for active continental margins, most prone to earthquakes. This conclusion is supported by a global study of crustal Poisson's ratios by Zandt and Ammon (1995), who reported that Mesozoic and Cenozoic belts have the lowest average crustal Poisson's ratios. Yet, the differences are small: Brocher's regression fit, Brocher's empirical fit, and Ludwig's empirical fit yield V_s values that differ on average by less than 0.05 km/sec (Fig. 2; Table 1).

Magistrale *et al.* (2000) use the Poisson's ratio versus ρ relation in Figure 4, published by Ludwig *et al.* (1970), to convert their 3D V_p model for southern California into a V_s model where their model does not have independent V_s control. Magistrale *et al.* (2000) perform this conversion after first converting their V_p model into a ρ model using the Nafe–Drake curve. The close similarity between Brocher's empirical fit and Ludwig's empirical fit (Figs. 2–4) means that they produce similar V_s models. Presenting these relations directly in terms of V_p (using either the mudline or Brocher's regression fit), however, permits direct conversion of V_p models into V_s models without requiring the intermediate step of converting them to ρ models.

A clear conclusion from this update is that for V_p up to 3.5 km/sec V_s increases and Poisson's ratio (and V_p/V_s) decreases rapidly with increasing V_p (Figs. 2, 3), as the ratio of the shear modulus (μ) to the first Lamé constant (λ) increases from 0 to 1. The rate of increase in V_s and decrease in Poisson's ratio is much more rapid than expected from some deep borehole measurements (Ohta *et al.*, 1977). The relations presented here lead to higher V_s and hence predict lower amplification of strong ground motions than either Ohta *et al.* (1977) or Brocher *et al.* (1997a) would predict. V_s values low enough to cause significant amplification of shear waves and surface waves, less than 1 km/sec (Joyner, 2000), would be expected only for units having a V_p less than about 2.4 km/sec (Fig. 2).

Mafic and calcium-rich rocks define a separate suite of rocks having a lower V_s and higher Poisson's ratio (Johnson and Christensen, 1992; Christensen, 1996; Mavko *et al.*, 1998), falling well below general trends (Fig. 2). Mafic rocks in this suite include basalts, diabase, and gabbros (Christensen, 1996) comprising ophiolites prevalent in northern California (Godfrey *et al.*, 1997). The calcium-rich rock suite includes dolomites, marbles, and anorthosites (Christensen, 1996), which are rare in northern California but more important globally. This study suggests that a separate V_p versus V_s relation, the mafic line, be used to fit these calcium-rich, mafic, and ophiolitic rocks (Table 3; Fig. 8B).

Pure serpentinite forms a third distinct cluster based on its low V_s, high Poisson's ratio ($\sigma = 0.34$), and low V_p and ρ (Christensen, 1966, 1996) (Figs. 2–4). These unusual physical properties (Godfrey *et al.*, 1997), along with their high magnetization (Saad, 1969), facilitate the remote detection of serpentinites (Blakely *et al.*, 2005).

Christensen and Mooney (1995) summarized the results of 560 global seismic refraction experiments to estimate the global average continental crustal thickness and V_p. They further subdivided the crust into orogens, shields and platforms, continental arcs, rifts, and extended crust, and provided estimates of the average crustal thickness and V_p for each type of crust. Brocher's regression fit, Brocher's empirical fit, or Ludwig's empirical fit can be used to estimate the average crustal V_s corresponding to these average crustal V_p. For the continental crust, Christensen and Mooney (1995) estimated an average crustal V_p of 6.44 km/sec; the corresponding average crustal V_s estimated from Brocher's regression fit (equation 6) is 3.75 km/sec. Similarly, for the five types of continental crust, Christensen and Mooney (1995) estimated average crustal V_p values between 6.21 and 6.44 km/sec; Brocher's regression fit (equation 6) predicts that the corresponding average crustal V_s values range between 3.64 and 3.75 km/sec. The average upper mantle refraction velocity, *Pn*, reported by Christensen and Mooney (1995), is 8.09 km/sec. Using either Brocher's empirical fit (equation 11) or Ludwig's empirical fit (equation 12) to calculate the corresponding average *Sn* yields 4.57 km/sec.

For most urban basins, the mudline (equation 7) likely provides the most direct and accurate estimate for V_s in saturated lithologies having a V_p between 1.49 and 4.25 km/sec. For the rest of the crust, having a V_p between 4.25 and 7.5 km/sec. Brocher's regression fit (equation 6) provides an accurate and the most direct estimate of V_s. For V_p between 7.5 and 8.5 km/sec, corresponding to the lower crust and upper mantle, either Brocher's empirical fit (equation 11) or Ludwig's empirical fit (equation 12) provides less direct but more accurate estimates of V_s. The mafic line (equation 8) should be used for converting V_p to V_s for crustal units known to have mafic and certain calcium-rich lithologies.

Acknowledgments

Naomi Boness and Carl Wentworth provided digital versions of the borehole logs shown in Figures 6 and 7. Jeanne Hardbeck provided V_p and V_s values from her tomography from the Hayward fault. Michael Bevis, Naomi Boness, Bob Crosson, Bob Mereu, Donna Eberhart-Phillips, Jeanne Hardebeck, Harold Magistrale, Dave Okaya, and Tom Pratt reviewed earlier versions of this article. This research was funded by the Earthquake Hazard Program of the U.S. Geological Survey.

References

Baise, L. G., D. S. Dreger, and S. D. Glaser (2003). The effect of shallow San Francisco Bay sediments on waveforms recorded during the M_w 4.6 Bolinas, California, earthquake, *Bull. Seism. Soc. Am.* **93,** 465–479.

Birch, F. A. (1966). Compressibility: elastic constants, in *Handbook of Physical Constants*, S. P. Clark (Editor), Geol. Soc. Am. Mem, Vol. 97, 97–173.

Blakely, R. J., T. M. Brocher, and R. A. Wells (2005). Subduction-zone magnetic anomalies and implications for hydrated upper mantle, *Geology* **33,** 445–448.

Boatwright, J., L. Blair, R. Catchings, M. Goldman, F. Perosi, and C. Steedman (2004). Using twelve years of USGS refraction lines to calibrate the Brocher and others (1997) 3D velocity model of the Bay Area, *U.S. Geol. Surv. Open-File Rept. 2004-1282*, 34 pp.

Boness, N. L., and M. D. Zoback (2004). Stress-induced seismic velocity

and physical properties in the SAFOD Pilot Hole in Parkfield, CA, *Geophys. Res. Lett.* **31,** L15S17, doi 10.1029/2003GL019020.

Boore, D. M. (2003). A compendium of *P*- and *S*-wave velocities for surface-to-borehole logging: summary and reanalysis of previously published data and analysis of unpublished data, *U.S. Geol. Surv. Open-File Rept. 03-191*, 14 pp., http://geopubs.wr.usgs.gov/open-file/of03-191/ (last accessed October 2005).

Brocher, T. M. (2005). A regional view of urban sedimentary basins in northern California based on oil industry compressional-wave velocity and density logs, *Bull. Seism. Soc. Am.* **95,** 2093–2114.

Brocher, T. M., and N. I. Christensen (2001). Density and velocity relationships for digital sonic and density logs from coastal Washington and laboratory measurements of Olympic Peninsula mafic rocks and greywackes, *U.S. Geol. Surv. Open-File Rept. 01-264*, 39 pp., http://geopubs.wr.usgs.gov/open-file/of01-264/ (last accessed October 2005).

Brocher, T. M., E. E. Brabb, R. D. Catchings, G. S. Fuis, T. E. Fumal, R. A. Jachens, A. S. Jayko, R. E. Kayen, R. J. McLaughlin, T. Parsons, M. J. Rymer, R. G. Stanley, and C. M. Wentworth (1997a). A crustal-scale 3-D seismic velocity model for the San Francisco Bay area, California, *Eos Trans. AGU* 78, no. 46, (suppl.), F435-436.

Brocher, T. M., G. S. Fuis, W. J. Lutter, N. I. Christensen, and N. A. Ratchowski (2004). Seismic velocity models for the Denali fault zone along the Richardson Highway, Alaska, *Bull. Seism. Soc. Am.* **94,** S85–S106.

Brocher, T. M., A. L. Ruebel, and E. E. Brabb (1997b). Compilation of 59 sonic and density logs from 51 oil test wells in the San Francisco Bay area, California, *U.S. Geol. Surv. Open-File Rept. 97-687*, 74 pp.

Castagna, J. P., M. L. Batzle, and R. L. Eastwood (1985). Relationships between compressional-wave and shear-wave velocities in clastic silicate rocks, *Geophysics* **50,** 571–581.

Christensen, N. I. (1966). Elastic velocity of basic rocks, *J. Geophys. Res.* **71,** 5921–5931.

Christensen, N. I. (1978). Ophiolites, seismic velocities and oceanic crustal structure, *Tectonophysics* **47,** 131–157.

Christensen, N. I. (1996). Poisson's ratio and crustal seismology, *J. Geophys. Res.* **101,** 3139–3156.

Christensen, N. I., and W. D. Mooney (1995). Seismic velocity structure and composition of the continental crust: a global view, *J. Geophys. Res.* **100,** 9761–9788.

Daley, T. M., and T. V. McEvilly (1990). Shear-wave anisotropy in the Parkfield Varian Well VSP, *Bull. Seism. Soc. Am.* **80,** 857–869.

De, G. S., D. F. Winterstein, and M. A. Meadows (1994). Comparison of *P*- and *S*-wave velocities and Q's from VSP and sonic log data, *Geophysics* **59,** 1512–1529.

Fletcher, J. B., J. Boatwright, and A. G. Lindh (2003). Wave propagation and site response in the Santa Clara Valley, *Bull. Seism. Soc. Am.* **93,** 480–500.

Fliedner, M. M., S. L. Klemperer, and N. I. Christensen (2000). Three-dimensional seismic model of the Sierra Nevada arc, California, and its implications for crustal and upper mantle composition, *J. Geophys. Res.* **105,** 10,899–10,921.

Frankel, A., and J. E. Vidale (1992). A three-dimensional simulation of seismic waves in Santa Clara Valley, California, from a Loma Prieta aftershock, *Bull. Seism. Soc. Am.* **82,** 2045–2074.

Gardner, G. H. F., L. W. Gardner, and A. R. Gregory (1974). Formation velocity and density—the diagnostic basics for stratigraphic traps, *Geophysics* **39,** 770–780.

Godfrey, N. J., B. C. Beaudoin, S. L. Klempererthe Mendocino Working Group USA, and S. L. Klemperer (1997). Ophiolitic basement to the Great Valley forearc basin, California, from seismic and gravity data: implications for crustal growth at the North American continental margin, *Geol. Soc. Am. Bull.* **109,** 1536–1562.

Hardebeck, J. L., A. J. Michael, and T. M. Brocher (2004). Seismic velocity structure and seismotectonics of the Hayward fault system, east San Francisco Bay, California, *Eos Trans. AGU*, **85,** no. 47, (suppl.), abstract S34A-05.

Jachens, R. C., R. F. Sikora, E. E. Brabb, C. M. Wentworth, T. M. Brocher, M. S. Marlow, and C. W. Roberts (1997). The basement interface: San Francisco Bay area, California, 3-D seismic model, *Eos Trans. AGU*, **78,** no. 46 (suppl.), F436.

Johnson, J. E., and N. I. Christensen (1992). Shear wave reflectivity, anisotropies, Poisson's ratios, and densities of a southern Appalachian Paleozoic sedimentary sequence, *Tectonophysics* **210,** 1–20.

Joyner, W. B. (2000). Strong motion from surface waves in deep sedimentary basins, *Bull. Seism. Soc. Am.* **90,** S95–S112.

Ludwig, W. J., J. E. Nafe, and C. L. Drake (1970). Seismic refraction, in *The Sea*, A. E. Maxwell (Editor), Vol. 4, Wiley-Interscience, New York, 53–84.

Magistrale, H., S. Day, R. W. Clayton, and R. Graves (2000). The SCEC Southern California reference three-dimensional seismic velocity model Version 2, *Bull. Seism. Soc. Am.* **90,** S65–S76.

Majer, E., T. V. McEvilly, F. S. Eastwood, and L. R. Meyer (1988). Fracture detection using P-and S-wave vertical seismic profiling at The Geysers, *Geophysics* **53,** 76–84.

Martin, R. J. III, R. H. Price, P. J. Boyd, and J. S. Noel (1994). Bulk and mechanical properties of the Paintbrush Tuff recovered from Borehole USWS NRG-6: Data report, Sandia Report, SAND93-4020, UC-814, 92 pp.

Martin, R. J. III, R. H. Price, P. J. Boyd, and J. S. Noel (1995). Bulk and mechanical properties of the Paintbrush Tuff recovered from Borehole USWS NRG-7/7A: Data report, Sandia Report, SAND94-1996, UC-814, 93 pp.

Mavko, G., T. Mukerji, and J. Dvorkin (1998). *The Rock Physics Handbook: Tools for Seismic Analysis in Porous Media*, Cambridge University Press, Cambridge, U.K., 329 pp.

Newhouse, M. W., R. T. Hanson, C. M. Wentworth, R. R. Everett, C. F. Williams, J. C. Tinsley, T. E. Noce, and B. A. Carkin (2004). Geologic, water-chemistry, and hydrologic data from multiple-well monitoring sites and selected water-supply wells in the Santa Clara Valley, California, 1999–2003, *U.S. Geol. Surv. Scient. Invest. Rep. 2004-5250*, 142 pp.

Price, R. H., R. J. Martin III, and R. W. Haupt (1994). The effect of frequency on Young's modulus and seismic wave attenuation, Sandia Report, SAND92-0847, UC-814, 50 pp.

Saad, A. F. (1969). Magnetic properties of ultramafic rocks from Red Mountain, California, *Geophysics* **34,** 974–987.

Stidham, C., M. Antolik, D. Dreger, S. Larsen, and B. Romanowicz (1999). Three-dimensional structure influences on the strong motion wavefield of the 1989 Loma Prieta earthquake, *Bull. Seism. Soc. Am.* **89,** 1184–1202.

Telford, W. M., L. P. Geldart, R. E. Sheriff, and D. A. Keys (1976). *Applied Geophysics*, Cambridge University Press, Cambridge, U.K., 860 pp.

Tiballi, C. A., and T. M. Brocher (1998). Compilation of 71 additional sonic and density logs from 59 oil test wells in the San Francisco Bay area, California, *U.S. Geol. Surv. Open-File Rept. 98-615*, 131 pp.

Zandt, G., and C. J. Ammon (1995). Continental crust composition constrained by measurements of crustal Poisson's ratio, *Nature* **374,** 152–154.

U.S. Geological Survey
345 Middlefield Road
MS 977
Menlo Park, California 94025

Manuscript received 14 April 2005.